Desalination and Water Treatment
www.deswater.com
doi: 10.1080/19443994.2013.862023

53 (2015) 1177–1187
February

Taylor & Francis
Taylor & Francis Group

Artificial neural networks for modeling the reverse osmosis unit in a wastewater pilot treatment plant

A. Salgado-Reyna, E. Soto-Regalado*, R. Gómez-González, F.J. Cerino-Córdova, R.B. García-Reyes, M.T. Garza-González, M.M. Alcalá-Rodríguez

Facultad de Ciencias Químicas, Universidad Autónoma de Nuevo León, Ciudad Universitaria S/N, Ciudad Universitaria, San Nicolás de los Garza, Nuevo León CP 66451, Mexico
Email: edsoto1962@yahoo.com.mx

Received 25 July 2012; Accepted 29 September 2013

ABSTRACT

This paper presents experimental and modeling data from a membrane-based wastewater treatment (WWT) pilot plant. The effluents from various upstream steps of a can-manufacturing plant were combined and subjected to a pretreatment process, which consisted of coalescing filters, coagulation and gravity settling, and sand activated carbon and polishing filtration, and a pressure-driven membrane process, such as reverse osmosis (RO). The performance of the RO membrane was evaluated and experiments were conducted using continuous wastewater flow. The complete membrane separation scheme was validated with a closed loop cell through several experiments, in which the concentration of the antiscaling agent and the pH were varied to determine the optimal operational conditions. Detailed parametric studies for these continuous flow experiments were conducted, and the permeate flow rates in the RO membrane system were experimentally measured. The experimental flow data were correlated and analyzed using an artificial neural network (ANN). A four-layer feed-forward network with a back-propagation algorithm was used to train the ANN models. After the training process was completed, the experimental flow data was used to assess the prediction capabilities of the networks based on the RO permeate water flow rate. This research showed that the RO unit results in the acceptable removal of 96.1% of the total dissolved solids and a maximum effluent recovery close to 72%. The predicted and experimental flow data were well correlated, and a determination coefficient between 0.97 and 0.99 was achieved.

Keywords: Pilot plant; Reverse osmosis membrane; Parametric study; Modeling; Artificial neural network

1. Introduction

Every year, industries in Mexico and around the world drain hundreds of thousands of cubic meters of effluents from their processes. These effluents are due to a lack of reliable process models, a lack of implementation of water-saving techniques in discharges, and the inefficient use of new biological, chemical, and physicochemical treatments in combination with new, more efficient and affordable technologies [1–7].

Artificial neural networks (ANN) has been applied to predict the effluent quality as a function of the wastewater quality parameters, to estimate the

*Corresponding author.

behavior of the system at different conditions, and to predict the best operational conditions as a function of the influent quality parameters, such as the chemical oxygen demand (COD), the biological oxygen demand, and the total suspended solids (TSS) [8–13]. According to the recent literature, there are not reports using ANN to model an reverse osmosis (RO) membrane as part of a pilot plant used to treat wastewater from a can-manufacturing plant.

ANN is composed of a large number of single elements (neurons), which are connected to each other in different ways forming various types of neural networks. The multi-layer feed-forward neural network with a back-propagation algorithm for training is the most popular ANN and was used in this work. The neurons are arranged into three or more layers [14, 15]: input, hidden (which enable the network to address non-linear and complex correlations), and output layers [16].

The wastewater used in the experiments contained significant quantities of total dissolved solids (TDS), suspended solids, and grease. The current treatment process of this wastewater, described by Reynolds and Richards [17], exhibits low performance: only 40% of the total treatment plant effluent is recovered and reused.

In this work, pretreatment and membrane-based processes were proposed to treat the effluent of a can manufacturing plant. The pretreatment process includes coalescing filters, coagulation and flocculation reactor, settling tank, sand and activated carbon filters and polishing filters. The membrane-based process was using a pressure-driven membrane separation involving RO.

An ANN model was used to describe the permeate flow profiles at the RO system of the can-manufacturing pilot plant under continuous flow and different operating conditions. Thus, the aim of this research was to increase the reuse rate of wastewater by determining improved conditions for the pretreatment processes at the laboratory scale. In addition, these conditions will be used for the operation of the pilot plant with an RO membrane.

2. Materials and methods

2.1. Wastewater quality

Several effluent samples were collected from the can manufacturing plant and analyzed (see Table 1) using physical-chemical methods [18], such as NMX-AA-093-SCFI-2000 for conductivity, NMX-AA-008-SCFI-2000 for pH, NMX-AA-072-SCFI-2001 for Calcium, Magnesium and total hardness, NMX-AA-075-1982 for SiO_2, NMX-AA-034-SCFI-2001 for total solids (TS), TDS and TSS, NMX-AA-005-SCFI-2000 for grease and oils, and NMX-AA030-1981 for COD. Table 1 shows the quality characteristics of the raw effluent, where high values are mainly due to the lack of an effective filtration process in the current plant. In particular, the high concentrations of silicon oxide are due to the washing water used, which is obtained from an underground water body. In contrast, the high conductivity, TS and TDS values are related to the application of chemical additives during the can washing process. These quality characteristics of the effluent indicate that it cannot be reused in other washing steps or discharged through the drain without an appropriated treatment.

Table 1
Quality characteristics of the raw effluent from the can—manufacturing plant

Parameters	Values
Conductivity, micro ohm/cm	2,467
pH	8.35
Total hardness, mg/L as $CaCO_3$	71.6
Calcium hardness, mg/L as $CaCO_3$	36
Magnesium hardness, mg/L as $CaCO_3$	35.6
Silicon oxide, mg/L	258
Total solids, TS, mg/L	1862
Total dissolved solids, TDS, mg/L	1817
Total suspended solids, TSS, mg/L	45
Chemical oxygen demand, COD, mg/L	300

2.2. Pretreatment

Fig. 1 shows the diagram of the current design of the can-manufacturing wastewater treatment (WWT) plant, which does not allow reaching a reuse rate higher than 40%.

Fig. 2 shows the diagram of the proposed design for the WWT plant. A pilot plant with a capacity of 908.40 L/h was built based on this design for test and validation purposes. As can be seen this proposal includes RO unit and polishing filters, which allow reaching treated water with better quality characteristics [19–22]. The wastewater is pretreated before it is fed into the RO unit to reduce the values of some parameters, such as conductivity, total hardness, silicon oxide, TDS, and COD. Both oil and grease are removed from the wastewater through a coalescing filter system, which is the most efficient and cost-effective method to separate the surface and emulsified hydrocarbons in the effluent.

Before the water stream enters the coagulation reactor, a continuous feed flow of coagulant and

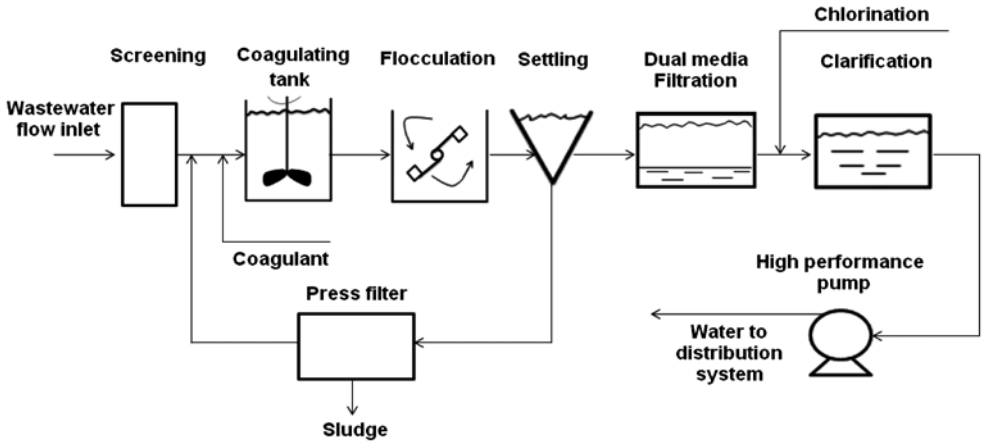

Fig. 1. Reynolds and Richards's high-speed sand filtration plant.

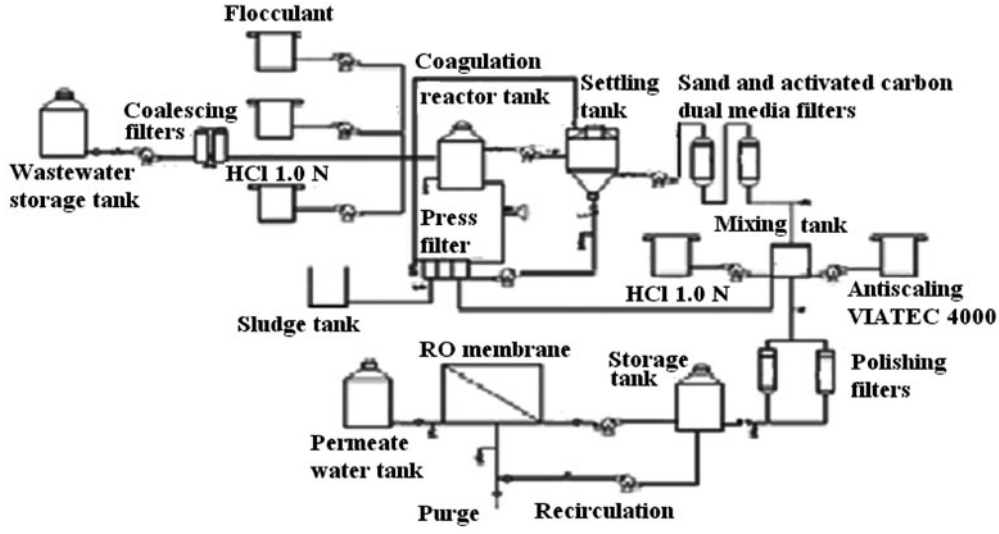

Fig. 2. Flowchart of the proposed WWT pilot plant.

flocculant were added, and the pH was maintained at 5 by the addition of a 1.0 N HCl acid solution. Different combinations of coagulant–flocculant were proposed and analyzed using a jar test.

The operational conditions for the coagulant reactor were determined during the same jar test using a 2^n factorial design, in which four variables (initial pH, coagulant concentration, stirring speed during flocculant addition, and flocculant concentration) and two levels for each variable (high and low) were considered. The best coagulant–flocculant combination was chosen based on the response variables (turbidity, absorptivity, and transmittance parameters).

The wastewater leaving the coagulation reactor is fed into a settling tank with a volume capacity of 1,100 L, where settling time was obtained using a batch settling column test. Additionally, the flow is fed into an array of two filters: a sand and gravel column and an activated carbon and anthracite column. These filters remove most of the suspended particles and organic compounds present in the effluent. Both columns have a height of 1.52 m and a total bed volume of 226.53 L.

After passing through the filter units, the effluent flows into a transfer tank, where it is mixed with an antiscaling solution (VIATEC 4000) with a concentration of 3.0 mg/L, and the pH is adjusted by the addition of 1.0 N HCl. The mixture is then fed to a polishing filter system in a parallel configuration. Each polishing column has a height of 0.53 m, a diameter of

0.10 m, and an area of 0.51 m^2 of poly propylene as the filter media.

2.3. RO membrane

An organic polyamide membrane is used for the RO. To avoid an excess solid load over the RO membrane [23], the effluent is pretreated and filtered before passing through the membrane. All of the RO membranes used in the trials were procured from Nitto Denko Company. The kind of membrane used in this study had the following characteristics: maximum operating pressure of 4.16 MPa, maximum chlorine concentration lower than 0.1 mg/L, maximum operation temperature of 45°C, range of operating pH from 2 to 10, turbidity in water lower than 1.0 NTU, minimum flux ratio concentrate/permeate of 5:1, maximum pressure drop equal to 0.07 MPa, and filtration area of 37.16 m^2.

2.4. Closed-loop RO membrane system

The RO membrane unit comprises a storage tank of 2,000 L and a subsequent high-pressure reciprocating pump, which discharges directly to the RO membrane and operates at a pressure of 1.87 MPa. The RO membrane cylinder has two outputs: one for the permeate flow and one for the recirculated flow (concentrate). The recirculate flow has a drained outlet (purge). The recirculated flow returns to the storage tank of this process unit.

2.5. ANN modeling

The number of hidden layers and the number of neurons in hidden layer are problem-specific and can be selected through trial and error [24].

After training, two hidden layers with a particular number of neurons resulted with less error prediction and were thus selected for the network architecture, which also included three input variables and one output response. During the training of the neural network, only 33% of the total collected data were used. The complete data set consist of the following inputs: silicon oxide inlet concentration, TDS inlet concentration, and time. The output of the network is the permeate flow and the Levenberg–Marquardt algorithm was used for the training.

3. Results and discussion

This section is divided into four parts. In the first part, the data from the main pretreatment processes are reported and discussed. The experimental data are presented and discussed in the second part. In the third part, an ANN was used to predict the flow data for the RO membrane system under different conditions. Finally, a comparison of the operational results between the current WWT used in the can-manufacturing plant (original process design) and the WWT pilot plant (new design proposal) is shown in the last part.

3.1. Wastewater pretreatment

Although the overall pretreatment stage comprises several processes, coagulation, flocculation, and sedimentation are the most important because these can have a direct influence on the performance of the RO unit.

3.1.1. Coagulation/flocculation trials

Table 2 shows the combinations of coagulants and flocculants used in these experiments. To determine the optimal conditions for coagulation and flocculation [25], a jar test [26] was performed at 22.6°C using the experimental trials showed in Table 3, and considering these results the best combination of coagulant and flocculants was selected.

The best combination of chemicals in Table 2 was found to be the number 2, with $Al_2(SO_4)_3$ as the coagulant and NALCO 9907 as the flocculant. This combination was tested in 16 trials, which were defined by the 2^4 factorial design, with two levels (high and low) for the initial pH, the coagulant concentration, the flocculant concentration, and the stirring speed during flocculant addition.

As shown in Table 3, the trial 16 was found to be the best based on the improved turbidity, absorptivity, and transmittance results, and the operating conditions that provided the best results were the following: pH controlled in 5, coagulant concentration of

Table 2
Coagulant–flocculant combinations used in the different jars tests

Combination	Coagulant	Flocculant
1	CaO	NALCO 9907
2	$Al_2(SO_4)_3$	NALCO 9907
3	$FeCl_3$	NALCO 9907
4	CaO	NALCO 3249
5	$Al_2(SO_4)_3$	NALCO 3249
6	$FeCl_3$	NALCO 3249

*NALCO is a worldwide chemical water treatment company.

Table 3
Jars testing results for case 2 with $Al_2(SO_4)_3$ as coagulant and NALCO 9907 as flocculant

Trial	Initial pH	Coagulant $Al_2(SO_4)_3$ 10.0 mg/L (mL)	RPM's 45 s	Cationic flocculant NALCO 9907, 1 mg/L (mL)	Final pH	Turbidity NTU	ABS ($\times 10^1$)	T%
1	10	1.00	100.00	1	9.78	1.00	0.03	99.34
2	5	6.50	150.00	4	6.01	2.00	0.10	97.65
3	5	1.00	100.00	1	5.61	1.00	0.06	98.70
4	10	6.50	100.00	1	9.72	4.00	0.17	96.23
5	10	1.00	150.00	4	9.58	2.00	0.09	98.00
6	10	1.00	100.00	4	9.80	1.00	0.04	99.06
7	10	6.50	100.00	4	9.81	0.00	0.00	100.0
8	10	6.50	150.00	4	9.59	1.00	0.04	99.20
9	10	6.50	150.00	1	9.78	4.00	0.19	95.69
10	10	1.00	150.00	1	9.77	2.00	0.07	98.47
11	5	6.50	150.00	1	5.93	5.00	0.22	95.06
12	5	6.50	100.00	1	5.59	1.00	0.04	99.08
13	5	1.00	150.00	1	5.98	1.00	0.03	99.23
14	5	1.00	150.00	4	6.00	1.00	0.02	99.60
15	5	6.50	100.00	4	5.72	0.00	0.01	99.68
16	5	1.00	100.00	4	5.82	0.00	0.00	100.0

*NTU = Nephelometric Turbidity Unit, ABS = Absorptivity, and T% = Transmittance.

10.0 mg/L, stirring required during flocculant addition of 100 min during 45 s, and flocculant concentration of 1.0 mg/L.

3.1.2. Batch settling column test

To achieve an effective separation of the suspended solids after the coagulation-flocculation process, it is important to determine the detention time in the settling tank. Therefore, tests were performed in a batch settling column to determine the percentage of suspended solids in water samples withdrawn from the column ports at different heights and at selected times intervals [27]. The settling column, consist of an acrylic pipe with a height of 330 cm, a diameter of 15.24 cm, and six sampling ports located at 50 cm intervals.

The amount of solid removal, which was expressed as a percentage, was calculated for each sample based on the initial concentration of suspended solids and the concentration of solids in the withdrawn sample. Fig. 3 shows the isopercentage curves representing the removal of solids at different times and depths.

At a settling time of 60 min, 85.41% of the suspended solids were removed and complete removal of the suspended solids was experimentally confirmed with a turbidity of 0.00 NTU after settling tank (same turbidity value of trial 16 in jar test results shown in Table 3). In the same way, chemical analysis taken off after settling tank at the wastewater pilot plant confirmed that the total hardness was eliminated.

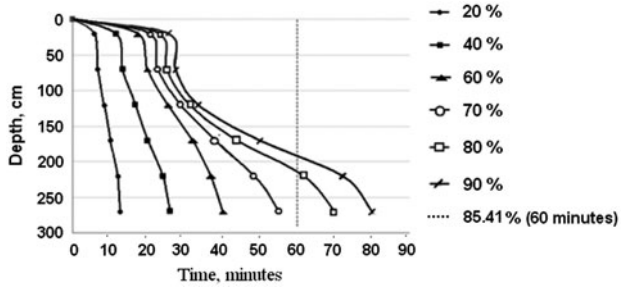

Fig. 3. Isopercentage curves for the calculation of the percentage removal of solids during the settling column test.

3.1.3. Antiscaling and pH adjustment

The effluent enters this transfer tank, where it is mixed with an antiscaling solution (VIATEC 4000) at a concentration of 3.0 mg/L and 1.0 N HCl, which is used for pH adjustment.

To determine the optimal operational conditions for the RO unit and to analyze the RO membrane fouling, several experiments with different pH and antiscaling agent concentrations were performed according to Table 4. Experiments 6 and 9 were performed under the same conditions but in experiment 9 the RO membrane being used was backwashed with a solution of 1.0 N HCl, whereas a new RO membrane was used in experiment 6.

Once the optimal conditions for the RO system were determined, several experimental runs were performed, and the resultant data were collected and

Table 4
Experimental analysis of the RO membrane system

Experiment	pH	Antiscaling agent (VIATEC 4000) concentration (mg/L)
1	12	1
2	7	1
3	12	3
4	7	3
5	4	1
6	4	3
7	3	1
8	3	3
9*	4	3

*In this particular case, the RO membrane was previously cleaned with HCl 1.0 N solution to reduce the pressure drop and increase the permeate flow.

analyzed using the ANN tool box in MATLAB R2009b [28–30].

3.2. Experimental data

Nine different runs were performed in the RO membrane system, as shown in Table 5. These results are shown in Figs. 4–8 for the nine different cases. As shown in Fig. 4, the SiO_2 concentration at the inlet of the RO membrane in all cases ranges from 18 to 22 mg/L and it is almost the same in all of the runs. Fig. 5 shows the SiO_2 concentration at the outlet of the RO membrane, which is constant at 4.0 mg /L for all cases, except for runs 1, 7, and 8.

Fig. 6 shows the TDS concentration at the RO membrane inlet, which ranges from 1,315 to 1,365 mg/L and is almost the same in all of the runs. Fig. 7 shows the TDS concentration at the outlet of the RO membrane, which shows a good reduction in all runs, but in cases 6 and 9 this TDS concentration reduction is better and ranges from 58 to 80 mg/L.

Fig. 8 shows the permeate water flow at the RO membrane for all runs and better performance is shown in case 9, which ranges from 499.62 to 681.30 L/h with an average of 647.24 L/h.

Table 5 shows the performance of the RO membrane after six days of continuous operation during the nine different cases, which involved different pH values and different concentrations of the antiscaling agent VIATEC 4000. Each experiment was run until the membrane became saturated, which caused the pressure drop to increase.

The results obtained for case 9 showed that 92.63 and 78.94% of the silicon oxides were removed in the treatment of the raw wastewater through the various processes prior to the RO separation process and

Table 5
RO membrane performance under different operation conditions

	Cases								
Variable	1	2	3	4	5	6	7	8	9
pH	12	7	12	7	4	4	3	3	4
Antiscaling agent concentration (mg/L)	1	1	3	3	1	3	1	3	3
Inlet SiO2 concentration (mg/L)	18	20	21	19	20	20	20	20	19
Inlet TDS concentration (mg/L)	1,380	1,343	1,302	1,311	1,350	1,351	1,339	1,341	1,346
Permeate water flow (L/h)	397.43	483.72	501.89	579.11	595.00	626.80	488.26	510.98	647.24
Outlet SiO2 concentration (mg/L)	4	4	4	4	4	4	10	6	4
Outlet TDS concentration (mg/L)	165	171	152	156	111	72	185	175	71

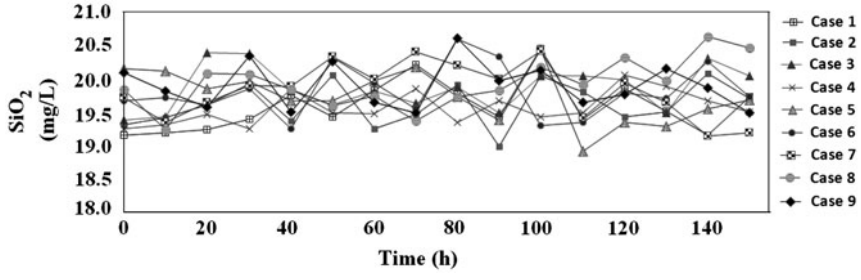

Fig. 4. SiO_2 concentration variation at the RO membrane inlet.

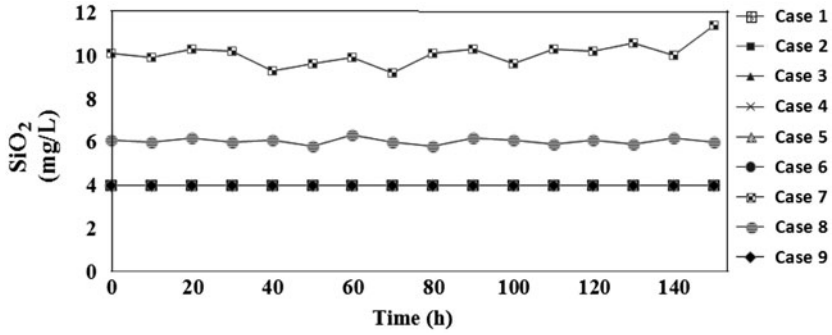

Fig. 5. SiO_2 concentration variation at the RO membrane outlet.

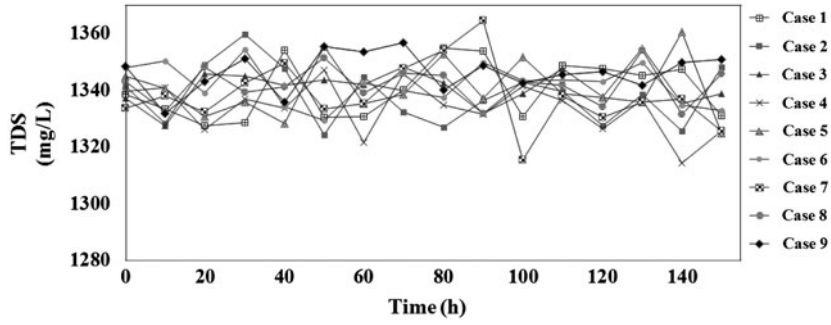

Fig. 6. TDS concentration variation at the RO membrane inlet.

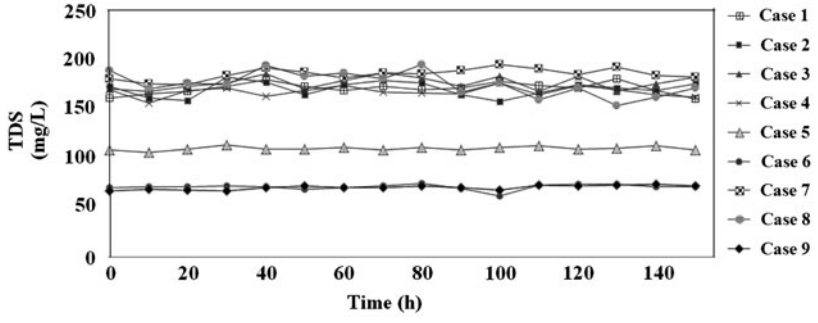

Fig. 7. TDS concentration variation at the RO membrane outlet.

through the RO membrane system, respectively, which indicates a global removal percentage of 98.44%. Additionally, removal percentages of 25.92 and 94.72% of the TDS were achieved in the same process steps, which result in a global TDS removal percentage of 96.09%.

These results confirm the contribution of the RO membrane system because TDS was not effectively removed by the coagulation-flocculation process. As shown in Table 5, the permeate flow shows a linear growth with increasing concentration of the antiscaling agent. In addition, decreasing the pH increased the permeate flow to its maximum, which was obtained at pH 4. In contrast, the TDS concentration exhibits a coupled relationship between the pH and the antiscaling agent concentration because it is not directly influenced by a single variable. The best behavior of the critical variables (permeate flow and

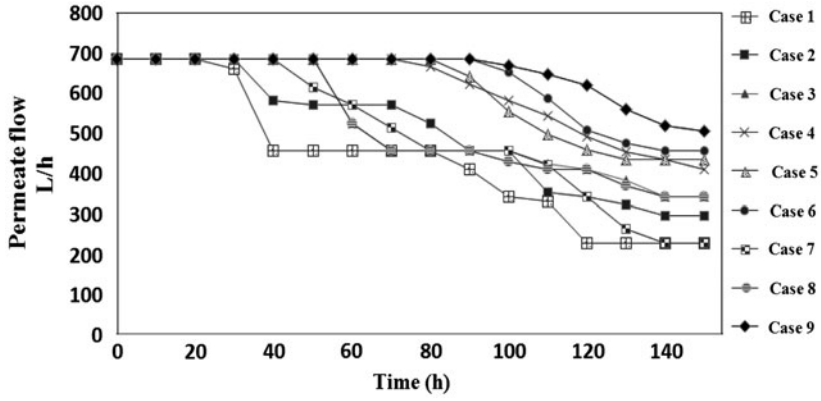

Fig. 8. Permeate water flow (L/h) at the RO membrane.

Table 6
ANN results for the experimental data obtained from all of the cases used to study the RO membrane system

Case	MSE ($\times 10^4$)	Number of iterations	Determination coefficient ($R^2 \times 10^1$)
1	72	181	9.87
2	171	143	9.75
3	322	21	9.56
4	7.34	574	9.97
5	5.78	29	9.98
6	2.38	171	9.98
7	242	56	9.86
8	345	55	9.64
9	5.55	27	9.97

TDS) was achieved at pH 4 and an antiscaling agent concentration of 3 mg/L (case 9 shown in Table 5). Thus, these conditions were used for the continuous operation of the pilot plant.

3.3. ANN modeling

Using the MATLAB ANN tool box, 33% of the 144 operational data sets collected (48 sets of operational data) were used for training, whereas 33% and 33% were used for validation and testing, respectively.

Table 6 shows the ANN results, including the mean square error (MSE), the number of iterations, and the determination coefficient, for the experimental data in the nine cases described in Table 5. For all of the cases, three neurons in each of hidden layers were considered, and the nets were trained using a Levenberg–Marquardt algorithm.

The goal of the training step is to minimize the error between the output y_k^p obtained by the network and the desired output, d_k^p. This error function, which is represented by E^p, is shown in Eq. (1):

$$E^p = \frac{1}{2}\sum_{k=1}^{M}\left(d_k^p - y_k^p\right)^2 \quad (1)$$

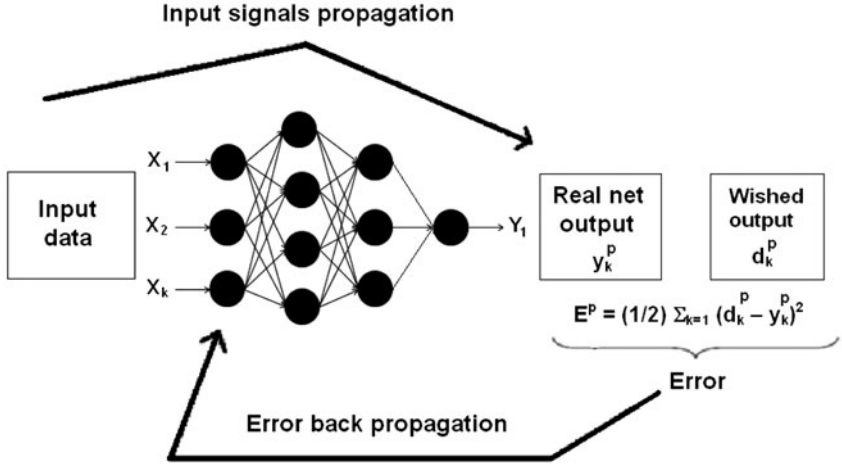

Fig. 9. Network architecture design used to obtain the best results for case 9.

where E^P = error function (see Figs. 2–8), d_k^P = the expected output in output neuron k and y_k^P = the real net output in output neuron k.

As shown in Table 5, the case nine gave the highest permeate flow and the lowest concentrations of silicone oxide and TDS at the RO membrane outlet after six days of continuous operation. In addition, the case nine results in one of the lowest MSE and one of the highest determination coefficients.

Fig. 9 shows the feed-forward network used for the analysis of the data obtained from case nine, which comprises three input variables, two hidden layers with four and three neurons, respectively (with the sigmoid-tangent transfer function), and one output response (with the sigmoid-logarithmic function). Different configurations of the ANN model were tested, with three neurons in the hidden layers, and one output response (with sigmoid-logarithmic function).

Table 7
ANN results using different networks for the experimental data obtained during case 9 in the test of the RO membrane system

Run	Network used	MSE ($\times 10^4$)	Number of iterations	Determination coefficient ($R^2 \times 10^1$)
1	Feedforward with Back propagation	5.64	25	9.98
2	Fitness approximation	2.38	170	9.75
3	Layered-recurrent	6.29	95	9.79
4	Pattern-recognition	2.81	25	Not determined

Table 8
ANN results using different network configurations for the experimental data obtained during case 9 in the test of the RO membrane system

Run	Number of neurons in the first hidden layer (*)	MSE ($\times 10^4$)	Number of iterations	Determination Coefficient ($R^2 \times 10^1$)
1	3	5.64	25	9.98
2	4	2.83	250	9.98
3	5	3.45	160	9.98
4	6	4.54	45	9.98
5	10	4.97	33	9.98

*Second hidden layer with 3 neurons in all runs.

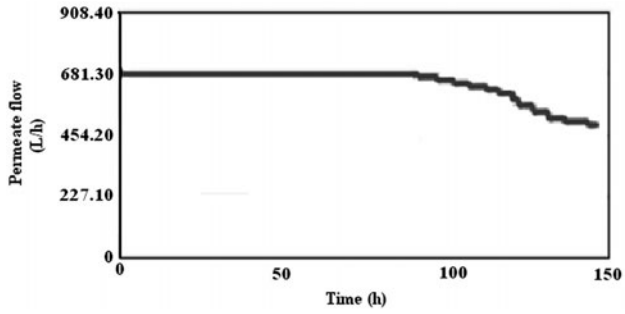

Fig. 10. Predicted and experimental values of the permeate water flow for all sets (case 9).

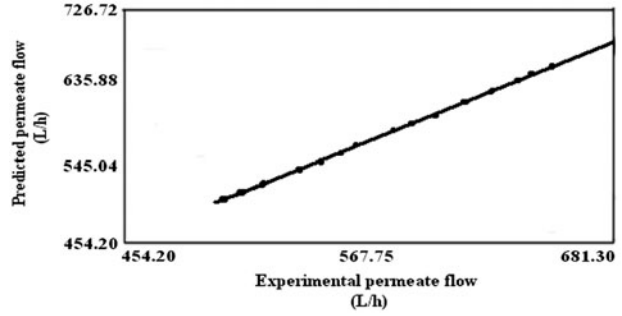

Fig. 11. Predicted and experimental values of the permeate water flow for all sets.

Table 7 shows the ANN results, including the network used, the MSE, the number of iterations, and the determination coefficient, for the experimental data obtained in case nine. Table 7 also shows that the feed-forward network selected (Newff) resulted in a very low MSE and the highest determination coefficient. The performance obtained in the selected network with different neural configurations is shown in Table 8.

The experimental and predicted decrease in the permeate flow at RO system is presented in Fig. 10. Fig. 11 compares the predicted and the experimental permeate flows and shows that the prediction is extremely close to the real values with a determination coefficient of 0.99.

3.4. Comparative analysis of the original and the proposed designs

The comparison of the complete operation of the WWT pilot plant (operation proposal) with the Reynolds and Richards's physical-chemical plant (original operation of the WWT in the can-manufacturing plant) is shown in Table 9.

Table 9
Comparison of the operational results obtained with the WWTP in the can-manufacturing plant (original process) and the WWT pilot plant (new design proposal)

Parameter	Units	Original process (Reynolds and Richards)	WWT Pilot plant	Improvement (%)
Conductivity	Micro mho/cm	119.70	65.80	45.02
pH	pH units	7.30	4	–
Total hardness	mg/L as $CaCO_3$	30	0	100
Calcium hardness	mg/L as $CaCO_3$	19	0	100
Magnesium hardness	mg/L as $CaCO_3$	11	0	100
Silicon oxide	mg/L	20	4	80
Total solids	mg/L	122	71	41.80
Total dissolved solids (TDS)	mg/L	122	71	41.80
Total suspended solids (TSS)	mg/L	0	0	0
Chemical oxygen demand (COD)	mg/L	50	<10	>80
Recovered and reused water flow	%	40	71.25	31.25

Table 9 shows that the operation of the pilot plant results in improvements in all of the reported parameters.

The main reasons of these improvements are the following: the use of coalescing filters, which maximized the elimination of grease and oils and improved the removal of COD, the adjustment of the pH to 4.0, which reduced bicarbonates and carbonates from pretreated wastewater and antiscaling addition helped to reduce the SiO_2 in the permeate water flow. The selection of the optimal coagulant and flocculant combination using jar test eliminated all types of hardness in the permeate water flow.

The inclusion of an RO membrane process in the pilot plant improved the wastewater filtration by decreasing the TS concentration. The combination of polishing filters with the use of the antiscaling agent VIATEC 4000 and pH adjustment, improved the operational cycle time of the RO membrane by significantly decreasing its fouling.

4. Conclusions

Effluents from a can-manufacturing plant were treated using a number of sequential pretreatment processes and membrane filtration. Pretreatment processes include coagulation, flocculation, settling and dual media sand-gravel, and activated carbon-anthracite filtration. Results of the coagulation and flocculation trials (based on the experimental design) show that effluents treated with $Al_2(SO_4)_3$ as coagulant and NALCO 9907 as a cationic flocculant, at pH 5, achieve the best quality of treated water (0 NTU). Furthermore, detention time of 1 h in the settling tank allows about 85% removal of the suspended solids. Moreover, to increase the permeate flow in the RO system and to avoid membrane fouling (measured as a high pressure drop), pH of the influent must be adjusted to 4, a dose of 3 mg/L of antiscaling agent must be added, and membrane must be operated at 1.87 MPa. At these conditions, the average permeate flow achieves the highest value (647.24 L/h) which represents a 71.25% water recovery with sufficient quality for reuse. These conditions also resulted in a reduction of 94.72% of the TDS and a reduction of 79% of the SiO_2 concentration.

The permeate flow rate was analyzed in different scenarios, and the possibility of an ANN approach was investigated. The optimal model, which consisted of a feed-forward network with two hidden layers with four and three neurons, respectively, was able to predict the permeate flow with the lowest MSE and a determination coefficient of 0.99. This developed model was able to interpolate the process variables at many other conditions of interest with excellent savings in both time and cost (as shown in cases 1 through 8). It is very important to mention that the wastewater pilot plant results in a significantly improved quality and quantity of the water treated and recuperated than the Reynolds and Richards technology used at the can manufacturing plant before of this investigation.

Acknowledgements

The experimental part of the present work was conducted in the Chemical Engineering Laboratory at UANL Chemical College and AQUAMEX WWT pilot plant at Monterrey and Toluca in Mexico, respectively.

The authors thank Dr Jorge Ibarra and Mr Alejandro Montes for allowing the experiments to be performed in their laboratories.

Symbols

E^P	—	error function
d_k^P	—	the expected output in output neuron k
y_k^P	—	the real net output in output neuron k

References

[1] G.W. Miller, Integrated concepts in water reuse: Managing global water needs, Desalination 187 (2006) 65–75.

[2] P.D. Saha, S. Dutta, Mathematical modeling of biosorption of safranin onto rice husk in a packed bed column using artificial neural network analysis, Desalin. Water Treat. 41 (2012) 308–314.

[3] M. Sadrzadeh, T. Mohammadi, J. Ivakpour, N. Kasiri, Neural network modeling of Pb^{2+} removal from wastewater using electrodialysis, Chem. Eng. Process.: Process Intensification, 48 (2009) 1371–1381.

[4] P.P. Pathe, A.K. Biswas, N.N. Rao, S.N. Kaul, Physicochemical treatment of wastewater from clusters of small scale cotton textile units, Environ. Technol. 26 (2005) 313–327.

[5] M. Gomez, F. Plaza, G. Garralon, J. Perez, M.A. Gomez, A comparative study of tertiary wastewater treatment by physic-chemical-UV process and macrofiltration-ultrafiltration technologies, Desalination 202 (2006) 369–376.

[6] T. Melin, B. Jefferson, D. Bixio, C. Thoeye, W. De Wilde, J. De Koning, J. Van der Graaf, T. Wintgens, Membrane bioreactor technology for wastewater treatment and reuse, Desalination 187 (2006) 271–282.

[7] J.R. Rao, N.K. Chandrababu, C. Muralidharan, B.U. Nair, P.G. Rao, T. Ramasamy, Recouping the wastewater: a way forward for cleaner leather processing, Cleaner Prod. 11 (2003) 591–599.

[8] M. Vyas, B. Modhera, V. Vyas, A.K. Sharma, Performance forcasting of common effluent treatment plant parameters by artificial neural network, ARPN. Eng. Appl. Sci. 6 (2011) 38–42.

[9] T.Y. Pai, Gray and neural network prediction of effluent from the wastewater treatment plant of industrial park, using influent quality, Environ. Eng. Sci. 25 (2008) 757–766.

[10] T.Y. Pai, Y.P. Tsai, H.M. Lo, C.H. Tsai, C.Y. Lin, Grey and neural network prediction of suspended solids and chemical oxygen demand in hospital wastewater treatment plant effluent, Comput. Chem. Eng. 31 (2007) 1272–1281.

[11] H.R. Tashaouie, G.B. Gholikandi, H. Hazrati, Artificial neural networks modeling for predict performance of pressure filters in a water treatment plant, Desalin. Water Treat. 39 (2012) 192–198.

[12] A.R. Khataee, Photocatalytic removal of C.I. Basic Red 46 on immobilized TiO_2 nanoparticles: Artificial neural network modeling, Environ. Technol. 30 (2009) 1155–1168.

[13] A. Kardam, K. Rohit Raj, J. Kumar Arora, M. Mohan Srivastava, S. Srivastava, Artificial neural network modeling for sorption of cadmium from aqueous system by shelled moringa oleifera seed powder as an agricultural waste, Water Res. Pr., 2 (2010) 339–344.

[14] M.B. Menhaj, Fundamentals of Neural Networks, Professor Hesabi Publications, Tehran, 1998.

[15] M.C. Bishop, Neural network and their applications, Rev. Sci. Instrum. 64 (1994) 1803–1831.

[16] I. Bardot, L. Bouchereau, N. Martin, B. Alagos, Sensory instrumental correlation by combining data analysis and neural network techniques, Food Qual. Pref. 51 (2) (1994) 159–166.

[17] T.D. Reynolds, P.A. Richards, Unit operations and processes in environmental engineering, PWS, Boston, MA, 1995.

[18] http://www.imta.gob.mx/cotennser/index.php?option=com_content&view=article&id=94&itemid=84

[19] M.S. Noghabi, S.M. Ali Razavi, S.M. Mousavi, Prediction of permeate flux and ionic compounds rejection of sugar beet press water nanofiltration using artificial neural networks, Desalin. Water Treat. 44 (2012) 83–91.

[20] Y.G. Lee, Y.S. Lee, J.J. Jeon, S. Lee, D.R. Yang, I.S. Kim, J.H. Kim, Artificial neural network model for optimizing operation of a seawater reverse osmosis desalination plant, Desalination 247 (2009) 180–189.

[21] V. Yangali-Quintanilla, A. Verliefde, T.-U. Kim, A. Sadmani, M. Kennedy, G. Amy, Artificial neural network models based on QSAR for predicting rejection of neural organic compounds by polyamide nanofiltration and reverse osmosis membranes, J. Membr. Sci. 342 (2009) 251–262.

[22] A. Cassano, R. Molinari, M. Romano, E. Drioli, Treatment of aqueous effluents of the leather industry by membrane processes: A review, J. Membr. Sci. 181 (2001) 111–126.

[23] L.G. Peeva, E. Gibbins, S.S. Luthra, L.S. White, R.P. Stateva, A.G. Livingston, Effect of concentration polarisation and osmotic pressure on flux in organic solvent nanofiltration, J. Membr. Sci. 236 (2004) 121–136.

[24] M. Khayet, C. Cojocaru, M. Essalhi, Artificial neural network modeling and response surface methodology of desalination by reverse osmosis, J. Membr. Sci. 368 (2011) 202–214.

[25] A.L. Ahmad, S. Ismail, S. Bathia, Optimization of coagulation—flocculation process for a palm oil mill effluent, using RSM, Environ. Sci. Technol. 39 (2005) 2828–2834.

[26] G.M. Fair, J.C. Geyer, D.A. Okun, Water and Wastewater Engineering, 3rd., John Wiley and Sons, 2008.

[27] Metcalf & Eddy Inc., Waste Water Engineering, Treatment and Reuse, Mc Graw Hill, New York, NY, 2003.

[28] Mathworks, MATLAB, Natick, MA, 2011.

[29] S.A. Martinez Delgadillo, M.G. Rodríguez Rosalez, Wastewater treatment with MATLAB (Tratamiento de aguas residuales con MATLAB), Editorial Reverté, Barcelona, 2005.

[30] B.M. del Brío, A.S. Molina, Neural Networks and Fuzzy Systems (Redes Neuronales y sistemas borrosos), Alfaomega Grupo editor, SA de CV, 2007.